Elastic and piezoelectric fields in substrates GaAs (001) and GaAs (111) due to a buried quantum dot

E. Pan[a)]
Structures Technology Incorporated, 543 Keisler Drive, Suite 204, Cary, North Carolina 27511

(Received 27 December 2001; accepted for publication 19 February 2002)

In this article we present a rigorous study on the elastic and piezoelectric fields in substrates GaAs (001) and GaAs (111) due to a buried quantum dot (QD) using an efficient and accurate continuum mechanics model. It is based on a Green's function solution in anisotropic and linearly piezoelectric half space combined with the generalized Betti reciprocal theorem. To address the effect of material anisotropy, two other substrates, Iso (001) and Iso (111), are also examined and they are assumed to be elastically isotropic. For a point QD with hydrostatic misfit strain $\gamma^* = 0.07$ in volume $v_a = 4\pi a^3/3$ where $a = 3$ nm, and at depth $h = 10$ nm below the surface, we have observed the following features. (1) The simplified elastically isotropic model should, in general, not be used for predicting elastic and piezoelectric fields in the semiconductor GaAs. (2) The magnitude of the QD-induced piezoelectric potential on the surface of GaAs (111) or GaAs (001) is comparable to, or even larger than, the direct potential. (3) Large horizontal and vertical electric fields, on the order of 10^6 V/m, can be induced on the surface of GaAs (001) and GaAs (111). (4) The elastic field induced on the surface of GaAs (001) has rotational symmetry of order C_4 (i.e., the elastic field remains the same after rotation of $2\pi/4$ around the [001] axis), while the corresponding piezoelectric field has rotational symmetry of order C_2. On the other hand, both the elastic and piezoelectric fields on the surface of GaAs (111) have rotational symmetry of C_3 around the [111] axis. (5) The magnitude of the elastic and piezoelectric quantities on the surface of GaAs (111) is, in general, larger than that of the corresponding quantities on the surface of GaAs (001). (6) Under different electric surface conditions (insulating or conducting), the surface piezoelectric fields induced are quite different. © *2002 American Institute of Physics.* [DOI: 10.1063/1.1468906]

I. INTRODUCTION

The self-assembled quantum dot (QD) structure possesses certain special electronic and optical features.[1,2] While achieving such a QD structure with the desired functionalities is still a great challenge to designing engineers and experimentalists, various computational methods have been proposed recently in order to offer a quantitative explanation of the QD structure through numerical modeling. The finite element method (FEM) and finite difference method (FDM), both domain-discretization methods, were usually applied.[2–5] Other methods include the two-dimensional Fourier transform method[6,7] and the atomistic quantum-mechanics model.[8,9]

In recent years, the Green's function related methods have been proposed and applied to QD modeling.[10] Because of its simple, accurate, and efficient features, the Green's function method has been found to be very useful.[7,10–13] A more recent advance in this method is the one proposed by Pan and Yang[14] that is based on the point-force Green's function solutions in an anisotropic and elastic half space[15] where they showed that both the material anisotropy and free surface could significantly influence the QD-induced elastic field.

A strained QD in a semiconductor induces not only an elastic field but also a piezoelectric field through polarization, and both fields are equally important to the electronic and optical properties of the related devices.[1,16] While the elastic field induced has been extensively studied, only a little research has been carried out on the corresponding piezoelectric field. Assuming a QD in an elastically isotropic and infinite GaAs substrate, Davies[12] derived analytically the induced piezoelectric potential and found that this potential is usually smaller than the corresponding direct potential (i.e., deformation potential times elastic strain). Using the FDM, Grundmann *et al.*[2] numerically solved the piezoelectric potential and studied other related electronic and optical properties of InAs/GaAs pyramidal QDs. Also using the FDM, Jogai recently calculated the elastic strain in coupled InAs/GaAs QDs[17] and the strain field and piezoelectric polarization charge in an InN/AlN wurtzite QD structure.[18] We point out that the piezoelectric quantities in either InAs/GaAs or InN/AlN were obtained based on a semi-coupled piezoelectric model. Recently, the author[19] proposed a fully coupled model and has shown that, in the calculation of QD-induced elastic and piezoelectric fields in the nitride III group where the electromechanical coupling is relatively strong, the fully coupled piezoelectric model must be used. Furthermore, based on the fully coupled model, the elastic and piezoelectric fields (e.g., elastic strain and electric field) can be solved simultaneously. In the semicoupled model, on the other hand, the elastic field is solved first, and the elastic field is then used as a driving force to solve the electric field induced. This sequential approach would be another disad-

[a)]Electronic mail: ernian_pan@yahoo.com

 © 2002 American Institute of Physics

Downloaded 13 May 2002 to 152.1.79.110. Redistribution subject to AIP license or copyright, see http://ojps.aip.org/japo/japcr.jsp

vantage should a numerical method, such as FEM or FDM, be used to solve the problem. It is apparent that the electric potential and electric field will be less accurate than the elastic field.

Besides the piezoelectric potential and polarization charge, the QD-induced electric field is also a very important factor in QD devices. In particular, this internally built-in electric field may be large enough to directly contribute to the Stark shift that should be considered in the design of electro-optic devices.[20–22] For semiconductor superlattices, the electric field induced by the lattice mismatch between the superlattice constituents has been analyzed often in the literature starting with the work by Smith.[23] It is well known that while no electric field exists on the surface of a superlattice made of GaAs and InAs with growth axis along [001], a large electric field can be induced on the surface of the corresponding superlattice with a growth axis along [111].[24,25] The question now is, What would the electric field be like on the surface of a substrate of GaAs (001) or GaAs (111) that is induced by a buried QD?

In this article, we apply a recently derived three-dimensional (3D) Green's function solution of the anisotropic and piezoelectric half space[19,26,27] to study QD-induced elastic and piezoelectric fields. This solution is based on the fully coupled model and can be equally applied to semiconductors in which the electromechanical coupling is relatively strong, like to the nitride III group. By using the point-force/point-charge Green's function and the generalized Betti reciprocal theorem, the QD-induced elastic and piezoelectric fields are expressed in terms of a simple integral on the surface of the QD for a finite-size QD, with the point-force/point-charge Green's function being the kernel. Furthermore, for a point QD, the elastic and piezoelectric fields can be directly expressed in terms of the point-force/point-charge Green's functions.

We then apply our Green's function solution to four substrates, namely, GaAs (001), GaAs (111), Iso (001), and Iso (111). The Iso (001) and Iso (111) models are similar to the GaAs (001) and GaAs (111), except for the elastic constants where, in Iso (001) and Iso (111), they are assumed to be isotropic. We calculate the elastic and piezoelectric fields on the surface of these substrates due to a buried point QD. For a point QD with a hydrostatic misfit strain $\gamma^* = 0.07$ in volume $v_a = 4\pi a^3/3$ where $a = 3$ nm, and depth $h = 10$ nm below the surface, we have observed the following important features.

(1) The simplified elastically isotropic model, in general, should not be used for the semiconductor GaAs. Otherwise, the elastic and piezoelectric fields predicted based on the isotropic model may be in error. It is clearly shown in this article that both the elastic and piezoelectric fields on the surfaces of the substrates GaAs and Iso can be substantially different and that replacing the cubic elastic constants in GaAs with the isotropic ones can render completely different results. For example, while the vertical electric field distribution on the surface of Iso (111) is completely rotational symmetric (i.e., the field is independent of the polar angle on the surface), it has rotational symmetry of order C_3 [i.e., it remains the same after a rotation of $2\pi/3$ around the [111] axis on the surface of GaAs (111)].

(2) Due to the existence of the traction-free, insulating surface boundary, the magnitude of the QD-induced piezoelectric potential on the surface of GaAs (111) or GaAs (001) is comparable to, or even larger than, the direct potential (i.e., the product of the elastic strain and deformation potential). This is different from in the infinite semiconductor case where the direct potential is usually larger than the piezoelectric potential.[12] In particular, the maximum magnitude of the QD-induced piezoelectric potential on the surface of GaAs (111) is 0.0476 V while the corresponding direct potential is 0.0523 eV, using a deformation potential of −7.17 eV for GaAs;[2] on the surface of GaAs (001), the maximum magnitude of the QD-induced piezoelectric potential can be even larger than the corresponding direct potential (0.0218 V vs 0.0156 eV). Therefore, this high magnitude of the piezoelectric potential, as well as of the direct potential, will contribute to a shift of the energy band, a feature that should be considered in the device of QD semiconductor heterostructures.

(3) Large horizontal and vertical electric fields, of the order of 10^6 V/m, can be induced on the surface of substrates GaAs (001) and GaAs (111); this is a magnitude similar to that observed on the surface of a superlattice made of InAs and GaAs with the growth axis along [111].[23] It should be noted that, for the superlattice case, no electric field exists on the surface of the superlattice made of InAs and GaAs with the growth axis along [001],[23] while for the QD case, a large electric field on the surface of GaAs (001), with magnitude of the same order as that on the surface of GaAs (111), can still be observed. This is a distinct feature between the quantum well and quantum dot structures, and it has not been discussed before as far as we know. Furthermore, a horizontal electric field as large as 0.48×10^7 V/m on the surface of GaAs (001) and one of 0.95×10^7 V/m on the surface of GaAs (111) have been observed. In a similar way, on the surface of GaAs (001) the vertical electric field can reach 0.26×10^7 V/m, and on the surface of GaAs (111) it can reach 1.20×10^7 V/m. These features are different from those observed on the surface of the corresponding superlattice, and should be of great interest to semiconductor device designers, particularly for optical modulators and self-electro-optical effect devices.

(4) While the QD-induced elastic field on the surface of the substrate GaAs (001) has rotational symmetry of order C_4, the corresponding piezoelectric field has only rotational symmetry of order C_2. On the other hand, both the elastic and piezoelectric fields have rotational symmetry of C_3 on the surface of the substrate GaAs (111).

(5) The magnitude of the elastic and piezoelectric quantities on the surface of GaAs (111) is, in general, larger than the magnitude of the corresponding quantities on the surface of GaAs (001).

(6) Under different electric surface conditions (insulating or conducting), the surface piezoelectric fields induced can

Downloaded 13 May 2002 to 152.1.79.110. Redistribution subject to AIP license or copyright, see http://ojps.aip.org/japo/japcr.jsp

be quite different, although different electric boundary conditions have no apparent influence on the elastic field because of the weak electromechanical coupling in GaAs.[19,27]

II. THEORY

For a fully coupled piezoelectric semiconductor, the constitutive relations can be expressed as[19,27]

$$\sigma_{ij}=C_{ijlm}\gamma_{lm}-e_{kji}E_k,$$
$$D_i=e_{ijk}\gamma_{jk}+\varepsilon_{ij}E_j, \tag{1}$$

where σ_{ij} and D_i are the stress and electric displacement, respectively, γ_{ij} is the strain and E_i the electric field, and C_{ijlm}, e_{ijk}, and ε_{ij} are the elastic moduli, piezoelectric coefficients, and dielectric constants, respectively. We point out that, in most previous studies, a semicoupled model was adopted in which the first constitutive relation of Eqs. (1) is used to solve the purely elastic field by dropping the second term on the right-hand side (i.e., $e_{ijk}=0$), and the second relation of Eqs. (1) is then used to find the piezoelectric field induced by the purely elastic field. It has been shown recently by the author[19,27] that when the electromechanical coupling in a semiconductor is weak, like in the III–V group, very accurate results can be obtained using the semicoupled model. However, if the electromechanical coupling in a semiconductor is relatively strong, like in AlN, one must use the fully coupled model. On the other hand, if the semiconductor shows clear anisotropy, a semicoupled model may not be able to simplify the problem. Therefore, in this article, the fully coupled model as expressed by Eqs. (1) is adopted.

Assuming a small deformation, the elastic strain and the electric field are then related to the elastic displacement u_i and electric potential ϕ as

$$\gamma_{ij}=\tfrac{1}{2}(u_{i,j}+u_{j,i}); \quad E_i=-\phi_{,i}. \tag{2}$$

We now apply the general piezoelectric constitutive relation, Eqs. (1), to the GaAs semiconductors. For GaAs (001) with crystalline axes [100], [010], and [001] along the x', y', and z' axes (i.e., the substrate coordinates x, y, and z are coincident with the crystalline axes), respectively, Eqs. (1) are reduced to

$$\begin{bmatrix}\sigma'_{xx}\\ \sigma'_{yy}\\ \sigma'_{zz}\end{bmatrix}=\begin{bmatrix}C'_{11} & C'_{12} & C'_{12}\\ C'_{12} & C'_{11} & C'_{12}\\ C'_{12} & C'_{12} & C'_{11}\end{bmatrix}\begin{bmatrix}\gamma'_{xx}\\ \gamma'_{yy}\\ \gamma'_{zz}\end{bmatrix}, \tag{3a}$$

$$\begin{bmatrix}\sigma'_{yz}\\ \sigma'_{xz}\\ \sigma'_{xy}\end{bmatrix}=2C'_{44}\begin{bmatrix}\gamma'_{yz}\\ \gamma'_{xz}\\ \gamma'_{xy}\end{bmatrix}-e'_{14}\begin{bmatrix}E'_{x}\\ E'_{y}\\ E'_{z}\end{bmatrix}, \tag{3b}$$

$$\begin{bmatrix}D'_{x}\\ D'_{y}\\ D'_{z}\end{bmatrix}=2e'_{14}\begin{bmatrix}\gamma'_{yz}\\ \gamma'_{xz}\\ \gamma'_{xy}\end{bmatrix}+\varepsilon_0\varepsilon'_r\begin{bmatrix}E'_{x}\\ E'_{y}\\ E'_{z}\end{bmatrix}, \tag{3c}$$

where a prime is added to the material properties as well as to the physical quantities to indicate that they are associated with the crystalline coordinates. It is interesting to observe that in the crystalline coordinates the normal stress and strain components are purely elastic. In other words, the piezoelectric field is coupled to the elastic shear stress and shear strain components only.

An elastically isotropic model, called Iso (001), is also used for a comparison study in which the elastic constants of GaAs (001) are replaced with its isotropic constants[14] while the piezoelectric and dielectric coefficients are exactly the same as those in GaAs (001).

For GaAs (111) with the substrate coordinates of the x axis along [11-2], the y axis along [−110], and the z axis along the [111] directions of the crystalline, the transformation matrix **A** from the crystalline coordinates (x', y', z') to the substrate coordinates (x, y, z) can be obtained using he following two sequential transforms:

$$\mathbf{A}=\begin{bmatrix}\cos\theta_2 & 0 & -\sin\theta_2\\ 0 & 1 & 0\\ \sin\theta_2 & 0 & \cos\theta_2\end{bmatrix}\begin{bmatrix}\cos\theta_1 & \sin\theta_1 & 0\\ -\sin\theta_1 & \cos\theta_1 & 0\\ 0 & 0 & 1\end{bmatrix}, \tag{4}$$

where

$$\theta_1=\pi/4; \quad \theta_2=\pi/2-\cos^{-1}(\sqrt{2/3}). \tag{5}$$

Therefore, with the matrix **A**, the global material properties can be found by the well-known tensor transformation.[28] It is seen that the relative dielectric constant will remain the same after transformation due to its isotropic property. However, the elastic constants and piezoelectric coefficients will change. In particular, the transformed piezoelectric matrix in the (x, y, z) coordinates for the substrate GaAs (111), using the common reduced notation, becomes

$$[e]=\begin{bmatrix}* & * & 0 & 0 & * & 0\\ 0 & 0 & 0 & * & 0 & *\\ * & * & * & 0 & 0 & 0\end{bmatrix}, \tag{6}$$

where the asterisk means a nonzero component. It is observed therefore that in the substrate GaAs (111), both the shear and normal strain components contribute to the piezoelectric field, while in the substrate GaAs (001), only the shear strain component contributes to the piezoelectric field, as can be seen clearly from Eqs. (3a)–(3c). We want to add that the difference between the [001] and [111] growth axes has been long noticed in the superlattice case where a large electric field in the superlattice made of GaAs and InAs with the growth axis along [111] can be induced by the mismatch strain between the constituents, while in the corresponding superlattice with the growth axis along [001] no electric field exists.[23]

Corresponding to the substrate GaAs (111), another elastically isotropic model, called Iso (111), is also used in which the elastic constants and the piezoelectric and dielectric coefficients are obtained from Iso (001) using the transformation matrix **A** given by Eq. (4). It is apparent that, since the elastic constants and dielectric coefficient are isotropic, they remain the same after transformation by Eq. (4). However, the piezoelectric coefficients will be transformed to a form similar to that of Eq. (6).

To sum up, therefore, there are four totally different models in this study: GaAs (001), GaAs (111), Iso (001), and

Downloaded 13 May 2002 to 152.1.79.110. Redistribution subject to AIP license or copyright, see http://ojps.aip.org/japo/japcr.jsp

Iso (111). In order to solve the elastic and piezoelectric fields, both the elastic and piezoelectric boundary conditions on the surface of the substrate need to be described. In this article, the following two types of boundary condition are considered. That is, at $z=0$,

$$\sigma_{xz}=0; \quad \sigma_{yz}=0; \quad \sigma_{zz}=0; \quad D_z=0, \tag{7a}$$

$$\sigma_{xz}=0; \quad \sigma_{yz}=0; \quad \sigma_{zz}=0; \quad \phi=0. \tag{7b}$$

It is seen that while Eq. (7a) corresponds to the traction-free insulating condition, Eq. (7b) corresponds to the traction-free conducting condition. In the following, the traction-free insulating condition is implied unless it is specified otherwise.

Let us assume now that there is eigenstrain within the substrate (modeled as a half space) and we would like to find the elastic and piezoelectric fields induced in the substrate. As has been shown recently for both the purely elastic and piezoelectric cases, the Green's function method is a very simple, accurate, and efficient method.[14,19] That is, the eigenstrain problem in an anisotropic and linearly piezoelectric half space can be solved in terms of an integral equation with the point-force/point-charge Green's functions being the kernels, a consequence of the generalized Betti reciprocal theorem. Assume that there is extended eigenstrain γ^*_{Ij} (i.e., γ^*_{ij} and E^*_i) in a finite subdomain Ω of the half space D; then the extended displacements (i.e., u_i and ϕ) are found to be[19]

$$u_K(\boldsymbol{y})=C_{iJLm}\gamma^*_{Lm}\int_{\partial\Omega}u^K_J(\boldsymbol{x};\boldsymbol{y})n_i(\boldsymbol{x})dS(\boldsymbol{x}), \tag{8}$$

where C_{iJLm} are the semiconductor's material properties including the elastic, piezoelectric, and dielectric coefficients,[19] and $n_i(\boldsymbol{x})$ are the outward normal components on the surface of Ω. The superscript K in Eq. (8) indicates the direction of the point force ($K=1$, 2, 3 for the point force) and the negative point charge ($K=4$).[19]

To find the misfit-strain induced extended strain field (i.e., γ_{ij} and E_i), we take the derivatives of Eq. (8) with respect to observation point $\boldsymbol{y}$ (or the source point of the point-force/point-charge Green's function), which yields

$$\gamma_{kp}(\boldsymbol{y})=\tfrac{1}{2}\gamma^*_{Lm}\int_{\partial\Omega}C_{iJLm}[u^k_{J,y_p}(\boldsymbol{x};\boldsymbol{y})+u^p_{J,y_k}(\boldsymbol{x};\boldsymbol{y})]n_j(\boldsymbol{x})dS(\boldsymbol{x}); \quad k=1,2,3, \tag{9a}$$

$$\gamma_{Kp}(\boldsymbol{y})=\gamma^*_{Lm}\int_{\partial\Omega}C_{iJLm}u^K_{J,y_p}(\boldsymbol{x};\boldsymbol{y})n_j(\boldsymbol{x})dS(\boldsymbol{x}); \quad K=4, \tag{9b}$$

with the corresponding extended stress field (i.e., σ_{ij} and D_i) being

$$\sigma_{iJ}(\boldsymbol{y})=C_{iJKp}[\gamma_{Kp}(\boldsymbol{y})-\chi\gamma^*_{Kp}], \tag{10}$$

where χ is equal to 1 if observation point $\boldsymbol{y}$ is within eigenstrain domain Ω, and is equal to 0 otherwise.

Finally, for a concentrated misfit strain applied at point $\boldsymbol{x}$, the elastic and piezoelectric fields induced can be expressed directly by the point-force/point-charge Green's functions. Assuming volume v_a for the QD at $\boldsymbol{x}$, the elastic displacement/electric potential and the elastic strain/electric field induced are found to be, respectively,

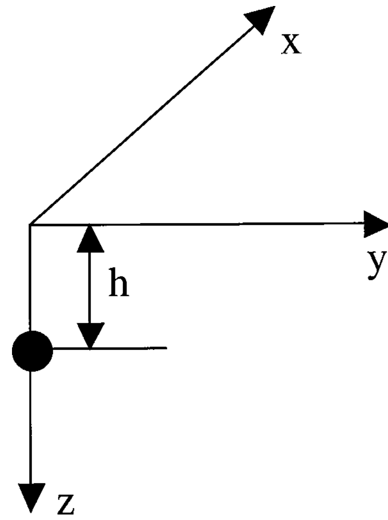

FIG. 1. Buried point quantum dot of volume $v_a=4\pi a^3/3$ at depth h below the surface of a half space where $a=3$ nm and $h=10$ nm. The misfit strain is $\gamma=0.07$.

$$u_K(\mathbf{y})=\sigma^K_{mL}(\boldsymbol{x};\boldsymbol{y})\gamma^*_{Lm}v_a \tag{11}$$

and

$$\gamma_{kp}(\mathbf{y})=\tfrac{1}{2}\gamma^*_{Lm}[\sigma^k_{mL,p_y}(\boldsymbol{x};\boldsymbol{y})+\sigma^p_{mL,k_y}(\boldsymbol{x};\boldsymbol{y})]v_a; \quad k=1,\ 2,\ 3, \tag{12a}$$

$$\gamma_{Kp}(\mathbf{y})=\gamma^*_{Lm}\sigma^K_{mL,p_y}(\boldsymbol{x};\boldsymbol{y})v_a; \quad K=4. \tag{12b}$$

It is interesting to observe from Eq. (11) that an eigenstrain (elastic strain/electric field)-induced displacement (elastic displacement/electric potential) can be expressed by the point-force/point-charge Green's stresses (elastic stress/electric displacement), similar to a general equivalent property between a point-force and a point-dislocation solution.[29,30]

III. RESULTS

The Green's function solutions, Eqs. (11) and (12), are now applied to the case of a buried point QD with volume $v_a=4\pi a^3/3$ in a substrate made of elastically isotropic material or of GaAs. The QD is located at depth h below the surface (Fig. 1) and the misfit strain is hydrostatic, i.e., $\gamma^*_{Ij}=\gamma^*\delta_{ij}$. In the following calculation, we assume that $h=10$ nm, $a=3$ nm, and $\gamma^*=0.07$. The elastic properties of GaAs (001) are $C'_{11}=118\times10^9$ N/m^2, $C'_{12}=54\times10^9$ N/m^2, and $C'_{44}=59\times10^9$ N/m^2.[7,14,31] For the elastically isotropic Iso (001), the elastic constants are $C'_{12}=54\times10^9$ N/m^2, $C'_{44}=59\times10^9$ N/m^2, and $C'_{11}=172\times10^9$ N/m^2, where C'_{11} is obtained by imposing the isotropic condition $C'_{11}-C'_{12}-2C'_{44}=0$.[14] The piezoelectric constant and relative permeability of GaAs (001) are, respectively, $e'_{14}=-0.16$ C/m^2 and $\varepsilon'_r=12.5$,[2] which are also used for the Iso (001) model. The material properties of substrate GaAs (111) and

Downloaded 13 May 2002 to 152.1.79.110. Redistribution subject to AIP license or copyright, see http://ojps.aip.org/japo/japcr.jsp

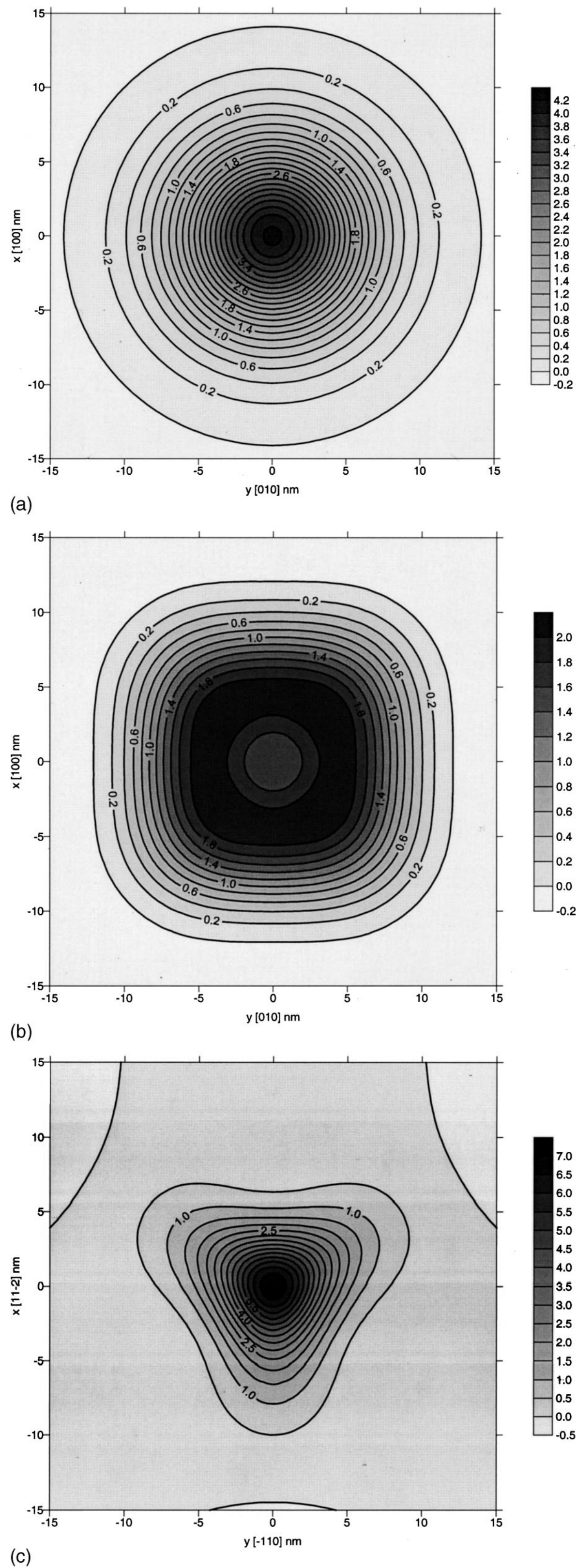

FIG. 2. (a) Contours of the hydrostatic strain $\gamma_{kk}(10^{-3})$ on the surface of the isotropic crystal due to a point quantum dot of volume v_a applied at distance $h=10$ nm. (b) Contours of the hydrostatic strain $\gamma_{kk}(10^{-3})$ on the surface of GaAs (001) due to a point quantum dot of volume v_a applied at distance $h=10$ nm. (c) Contours of the hydrostatic strain $\gamma_{kk}(10^{-3})$ on the surface of GaAs (111) due to a point quantum dot of volume v_a applied at distance $h=10$ nm.

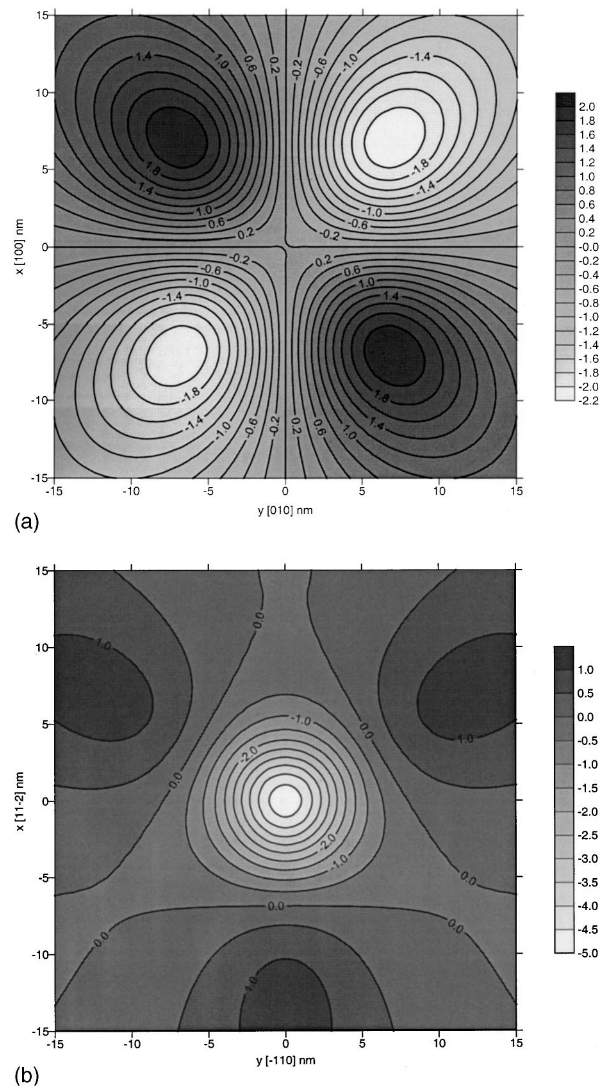

FIG. 3. (a) Contours of the electric potential $\phi(10^{-2}\ \mathrm{V})$ on the surface of GaAs (001) due to a point quantum dot of volume v_a applied at distance $h=10$ nm. (b) Contours of the electric potential $\phi(10^{-2}\ \mathrm{V})$ on the surface of GaAs (111) due to a point quantum dot of volume v_a applied at distance $h=10$ nm.

of elastically isotropic Iso (111) are obtained, respectively, from GaAs (001) and Iso (001), using transformation, Eq. (4). Again, unless specified, the traction-free insulating surface condition, Eq. (7a), is imposed.

Shown in Figs. 2(a)–2(c) are, respectively, contours of hydrostatic strain γ_{kk} on the surface of substrates Iso (001), GaAs (001), and GaAs (111) due to the buried point QD described above. It should be mentioned that, since the electromechanical coupling is weak for these materials,[19,27] the hydrostatic strain in Iso (111) is similar to that in Iso (001), both of which show completely rotational symmetry about the z axis (i.e., it is independent of the polar angle on the surface). On the surface of GaAs (001), however, the hydrostatic strain has the x axis, y axis, as well as the diagonal axes as its symmetric axes. In other words, the hydrostatic strain has rotational symmetry of order C_4. Namely, the hydrostatic strain remains the same after a rotation of $2\pi/4$ around the [001] axis. Furthermore, on the surface of GaAs (111), the contour shape of the hydrostatic strain is completely dif-

Downloaded 13 May 2002 to 152.1.79.110. Redistribution subject to AIP license or copyright, see http://ojps.aip.org/japo/japcr.jsp

ferent from that in Iso (001) and GaAs (001), and has rotational symmetry of order C_3. It is interesting that the maximum hydrostatic strain reached on the surface of Iso (001), GaAs (001), and GaAs (111) is, respectively, 0.005, 0.002, and 0.007, or about 7%, 3%, and 10% of the misfit strain. Therefore, high hydrostatic strain is expected if the growth direction in GaAs is along the [111] axis. We further want to mention that other elastic fields on the surface of the Iso (001), GaAs (001), and GaAs (111), namely, the hydrostatic stress, elastic strain energy, and vertical elastic displacement, follow similar contour shapes as their corresponding hydrostatic strain. These features clearly indicate that the elastically isotropic model is not suitable for analysis of the QD-induced elastic field in the anisotropic semiconductor GaAs.[14] We will show next that the elastically isotropic model is not suitable in the analysis of the QD-induced piezoelectric field in GaAs either.

Plotted in Figs. 3(a) and 3(b) are, respectively, contours of the piezoelectric potential on the surface of substrates GaAs (001) and GaAs (111) due to the same point QD. We want to remark that the contours on the surface of the Iso (001) and Iso (111) are, respectively, similar (but not exactly the same!), to those in Figs. 3(a) and 3(b). Thus, the piezoelectric potential in GaAs (001) or in Iso (001) has rotational symmetry of order C_2.[12,19,21] The distribution of the piezoelectric potential on the surface of GaAs (111) or Iso (111), however, is quite different. Similar to the corresponding hydrostatic strain, it has rotational symmetry of order C_3. In particular, we emphasize that the piezoelectric potential on the surface of the (111)-oriented substrate is not completely rotational symmetric, even in the elastically isotropic Iso (111)! Another interesting feature is that the magnitude of the piezoelectric potential on the surface of the (111)-oriented substrate can be much larger than that on the surface of the corresponding (001)-oriented substrate, and that the piezoelectric potential on the surface of either substrate can reach a magnitude comparable to the corresponding direct potential (i.e., the deformation potential times the elastic strain). For example, using a deformation potential of $a_c = -7.17$ eV for GaAs,[2] we found that the maximum magnitude for the direct potential on the surface of GaAs (111) is 0.0523 eV while the corresponding piezoelectric potential is 0.0476 V. Therefore, in contrast to the infinite-space situation, the contribution from the piezoelectric potential to the conduction band shift cannot be neglected for the substrate case. Furthermore, on the surface of GaAs (001), the maximum direct potential is 0.0156 eV while the corresponding maximum piezoelectric potential is 0.0218 V, with the latter being even larger than the former! Finally, we observe that while in GaAs (111) both the maxima of the direct potential and piezoelectric potential are reached at the same surface point [see Figs. 2(c) and 3(b)], the maxima of the direct potential and piezoelectric potential in GaAs (001) are reached at different surface points [Figs. 2(b) and 3(a)].

Figures 4(a) and 4(b) depict, respectively, contours of the horizontal electric field $E_h = \sqrt{E_x^2 + E_y^2}$ on the surface of substrates GaAs (001) and GaAs (111). We want to mention again that the horizontal electric fields on the surface of Iso (001) and of Iso (111) have similar but slightly different contour distributions compared to those in Figs. 4(a) and 4(b), respectively. It is observed that, similar to the piezoelectric potential or the elastic quantities, the horizontal electric field in the (111)-oriented substrate is much larger than that in the (001)-oriented substrate, e.g., 0.95×10^7 V/m in GaAs (111) vs 0.40×10^7 V/m in GaAs (001). These large magnitudes of the horizontal electric fields are comparable to those observed on the surface of the superlattice made of GaAs and InAs with growth axis along [111]. We further want to remark that, for the superlattice case where the mismatch strain is uniform in the whole structure, the horizontal electric field is always zero if the growth direction is along the [001] axis.[23] Here, however, we have observed that, for the substrate GaAs (001), a magnitude for the horizontal electric field, about half that in the corresponding (111)-oriented substrate, can still be induced by the point QD.

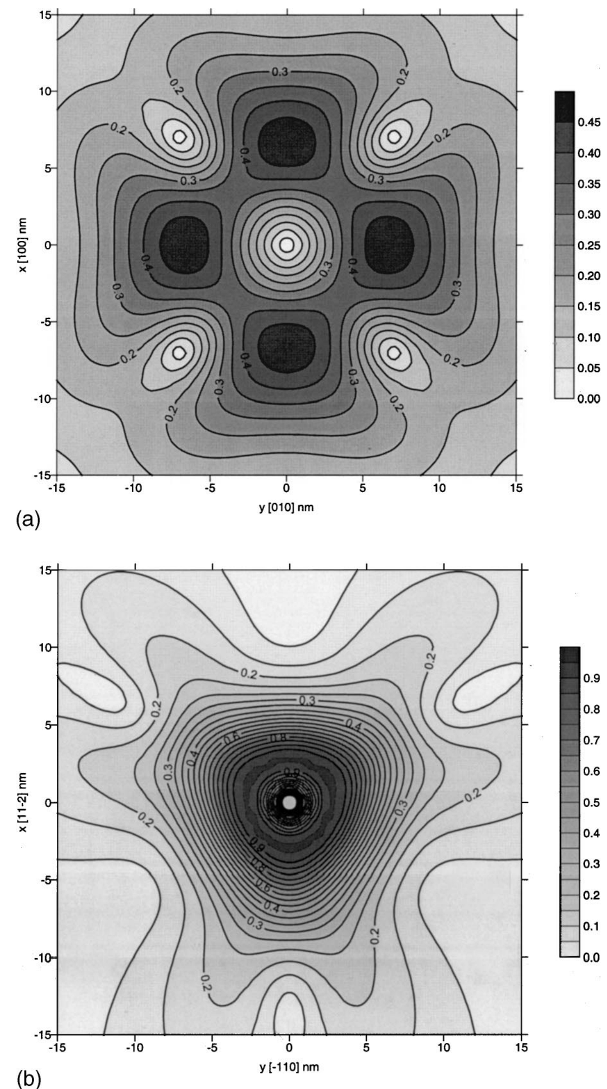

FIG. 4. (a) Contours of the horizontal electric field $E_h = \sqrt{E_x^2 + E_y^2} (10^7 \mathrm{V/m})$ on the surface of GaAs (001) due to a point quantum dot of volume v_a applied at distance $h = 10$ nm. (b) Contours of the horizontal electric field $E_h = \sqrt{E_x^2 + E_y^2}$ on the surface of GaAs (111) due to a point quantum dot of volume v_a applied at distance $h = 10$ nm.

Figures 5(a)–5(d) are contours of the vertical electric field E_z on the surface of substrates Iso (001), Iso (111),

Downloaded 13 May 2002 to 152.1.79.110. Redistribution subject to AIP license or copyright, see http://ojps.aip.org/japo/japcr.jsp

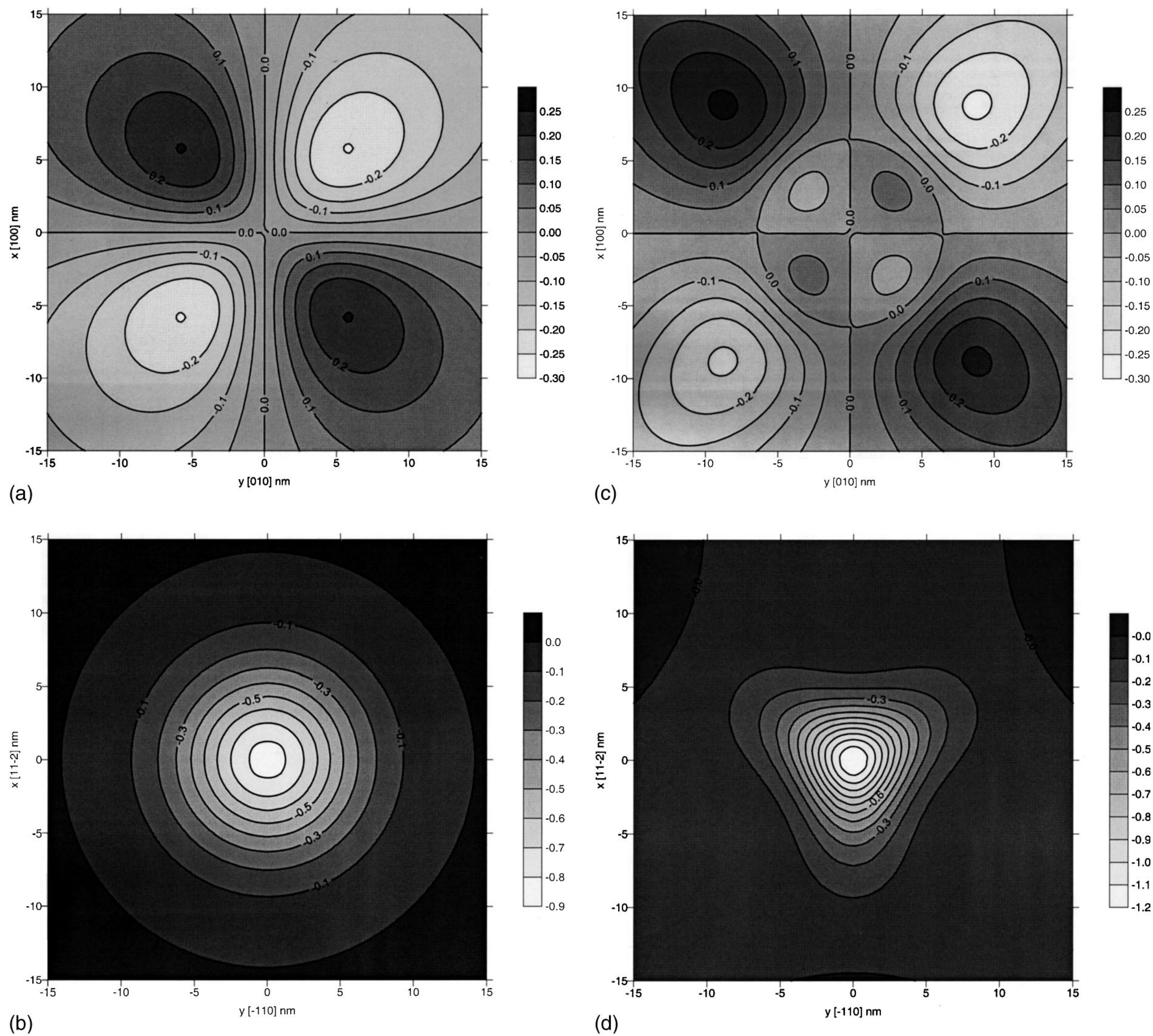

FIG. 5. (a) Contours of vertical electric field $E_z(10^7 \mathrm{V/m})$ on the surface of isotropic crystal (001) due to a point quantum dot of volume v_a applied at distance $h=10$ nm. (b) Contours of vertical electric field $E_z(10^7 \mathrm{V/m})$ on the surface of isotropic crystal (111) due to a point quantum dot of volume v_a applied at distance $h=10$ nm. (c) Contours of vertical electric field $E_z(10^7$ V/m) on the surface of GaAs (001) due to a point quantum dot of volume v_a applied at distance $h=10$ nm. (d) Contours of vertical electric field E_z on the surface of GaAs (111) due to a point quantum dot of volume v_a applied at distance $h=10$ nm.

GaAs (001), and GaAs (111). Notice that, unlike the horizontal electric field or the piezoelectric potential, the vertical electric field in GaAs (001) or (111) is quite different from that in Iso (001) or (111). While the vertical electric field in Iso (001) follows the same pattern of the corresponding piezoelectric potential in Iso (001), the vertical electric field in GaAs (001) is quite different from its corresponding piezoelectric potential distribution in GaAs (001) and also different from that in Iso (001). It is particularly interesting that the vertical electric field on the surface of GaAs (001) has two global maxima and minima and four local minor extremes inside [Fig. 5(c)]. While vertical electric field E_z is completely rotational symmetric in Iso (111), as observed by Davies[12] and by Bimberg *et al.*,[1] it has rotational symmetry of order C_3 in GaAs (111). Therefore, one should be particularly careful in applying the isotropic results to GaAs semiconductors, otherwise, a false conclusion may be reached. Again, like for other elastic and electric quantities, growth in the [111] axis can result in much larger elastic and electric quantities compared to those grown along the [001] axis. We finally want to add that both the horizontal and vertical electric fields on the surfaces of GaAs (001) and of GaAs (111) are on the order of 10^6 V/m, a magnitude that may be directly attributed to the recently observed Stark shift.[21]

All results presented so far are for the elastic traction-free and electric insulating boundary conditions. What will the elastic and piezoelectric fields be like should the insulating boundary condition be replaced by the conducting boundary condition? We already know that replacing the insulating boundary condition with the conducting condition has nearly no influence on the elastic field since electromechanical coupling is weak in GaAs.[19,27]

Figures 6(a) and 6(b) show, respectively, vertical electric field E_z on the conducting surfaces of substrates GaAs (001) and GaAs (111). It should be noted that the horizontal electric fields are zero on the surface due to fact that, on the

Downloaded 13 May 2002 to 152.1.79.110. Redistribution subject to AIP license or copyright, see http://ojps.aip.org/japo/japcr.jsp

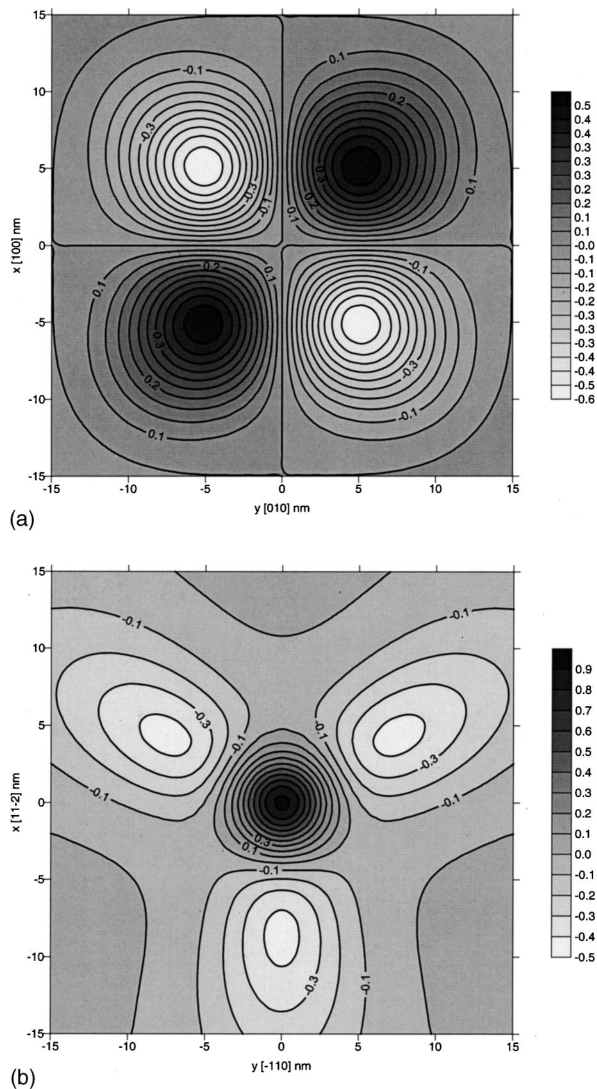

FIG. 6. (a) Contours of vertical electric field $E_z(10^7$ V/m) on the surface of GaAs (001) due to a point quantum dot of volume v_a applied at distance $h=10$ nm. Traction-free and isolating surface conditions are shown. (b) Contours of vertical electric field $E_z(10^7$ V/m) on the surface of GaAs (111) due to a point quantum dot of volume v_a applied at distance $h=10$ nm. Traction-free and isolating surface conditions are assumed.

conducting surface, $\phi=0$. In comparing Figs. 6(a) and 6(b) to Figs. 5(c) and 5(d), respectively, it is observed that vertical electric field E_z, in terms of shape and magnitude, can be completely different should a different electric surface condition be imposed. Therefore, different electric distributions may be induced by the buried QD if the insulating condition is replaced by a conducting one. Similarly, as was shown previously for the point-force case, a change in the mechanical boundary condition could also result in a totally different elastic field distribution.[27]

IV. CONCLUSIONS

In this article, a recently derived 3D Green's function in anisotropic and piezoelectric half space was used to study the QD-induced elastic and piezoelectric fields on the surface of an anisotropic semiconductor substrate. Using the generalized Betti reciprocal theorem, the eigenstrain problem is reduced to a simple surface integral with the point-force/point-charge Green's functions being the kernels. Numerical examples were then carried out for a buried point QD in anisotropic and piezoelectric substrates made of GaAs (001), GaAs (111), and elastically isotropic Iso (001) and Iso (111). Through these typical examples, details of the structure of the symmetry and magnitude of the elastic and piezoelectric fields were illustrated along with the following important features.

(1) The simplified elastically isotropic model, in general, should not be used for semiconductor GaAs, since the elastic and piezoelectric fields based on the isotropic model may be in error.
(2) The magnitude of the QD-induced piezoelectric potential on the surface of GaAs (111) or GaAs (001) is comparable to, or even larger than, the direct potential (i.e., the product of the elastic strain and the deformation potential).
(3) Large horizontal and vertical electric fields, on the order of 10^6 V/m, can be induced on the surface of GaAs (001) and GaAs (111), with magnitude similar to that obtained for the corresponding superlattice case.[23] It should be noted that, while for the superlattice case, no electric field exists on the surface with the growth axis along [001], for the QD case, however, the electric field does not vanish. Furthermore, the magnitude of the electric field on the surface of GaAs (001) is of the same order as that on the surface of GaAs (111), a feature distinct between the quantum well and quantum dot structures.
(4) While the elastic field induced on the surface of GaAs (001) has rotational symmetry of order C_4, the piezoelectric field induced has only rotational symmetry of order C_2. On the other hand, both the elastic and piezoelectric fields on the surface of GaAs (111) have rotational symmetry of C_3.
(5) The magnitude of the elastic and piezoelectric quantities in GaAs (111) is, in general, larger than that of the corresponding quantities in GaAs (001).
(6) Under different electric surface conditions (insulating or conducting), the surface piezoelectric fields induced can be quite different in both magnitude and shape.

[1] D. Bimberg, M. Grundmann, and N. N. Ledentsov, *Quantum Dot Heterostructures* (Wiley, New York, 1998).
[2] M. Grundmann, O. Stier, and D. Bimberg, Phys. Rev. B **52**, 11969 (1995).
[3] T. Benabbas, P. Francois, Y. Androussi, and A. Lefebvre, J. Appl. Phys. **80**, 2763 (1996).
[4] S. Kret, T. Benabbas, C. Delamarre, Y. Androussi, A. Dubon, J. Y. Laval, and A. Lefebvre, J. Appl. Phys. **86**, 1988 (1999).
[5] A. E. Romanov, G. E. Beltz, W. T. Fischer, P. M. Petroff, and J. S. Speck, J. Appl. Phys. **89**, 4523 (2001).
[6] V. Holy, G. Springholz, M. Pinczolits, and G. Bauer, Phys. Rev. Lett. **83**, 356 (1999).
[7] A. D. Andreev, J. R. Downes, D. A. Faux, and E. P. O'Reilly, J. Appl. Phys. **86**, 297 (1999).
[8] C. Pryor, J. Kim, L. W. Wang, A. J. Williamson, and A. Zunger, J. Appl. Phys. **83**, 2548 (1998).
[9] Y. Kikuchi, H. Sugii, and K. Shintani, J. Appl. Phys. **89**, 1191 (2001).
[10] D. A. Faux and G. S. Pearson, Phys. Rev. B **62**, R4798 (2000).
[11] J. R. Downes, D. A. Faux, and E. P. O'Reilly, J. Appl. Phys. **81**, 6700 (1997).

Downloaded 13 May 2002 to 152.1.79.110. Redistribution subject to AIP license or copyright, see http://ojps.aip.org/japo/japcr.jsp

[12] J. H. Davies, J. Appl. Phys. **84**, 1358 (1998), Appl. Phys. Lett. **75**, 4142 (1999).
[13] G. S. Pearson and D. A. Faux, J. Appl. Phys. **88**, 730 (2000).
[14] E. Pan and B. Yang, J. Appl. Phys. **90**, 6190 (2001).
[15] E. Pan and F. G. Yuan, Int. J. Solids Struct. **37**, 5329 (2000).
[16] J. Singh, *Physics of Semiconductors and their Heterostructures* (McGraw–Hill, New York, 1993).
[17] B. Jogai, J. Appl. Phys. **88**, 5050 (2000).
[18] B. Jogai, J. Appl. Phys. **90**, 699 (2001).
[19] E. Pan, J. Appl. Phys. **91**, 3785 (2002).
[20] S. Sanguinetti, M. Gurioli, E. Grilli, M. Guzzi, and M. Henini, Thin Solid Films **380**, 198 (2000).
[21] A. Patane, A. Levin, A. Polimeni, F. Schindler, P. C. Main, L. Eaves, and M. Henini, Appl. Phys. Lett. **77**, 2979 (2000).
[22] B. W. Kim, J. Appl. Phys. **89**, 1197 (2001).
[23] D. L. Smith, Solid State Commun. **57**, 919 (1986).
[24] D. L. Smith and C. Mailhiot, J. Appl. Phys. **63**, 2717 (1988).
[25] D. L. Smith and C. Mailhiot, Rev. Mod. Phys. **62**, 173 (1990).
[26] E. Pan and F. G. Yuan, Int. J. Eng. Sci. **38**, 1939 (2000).
[27] E. Pan, Proc. R. Soc. London, Ser. A **458**, 181 (2002).
[28] J. F. Nye, *Physical Properties of Crystals* (Clarendon, Oxford, 1985).
[29] E. Pan, Acta Mech. **87**, 105 (1991).
[30] A. H. D. Cheng and E. Detournay, Int. J. Solids Struct. **35**, 4521 (1999).
[31] M. P. C. M. Krijn, Semicond. Sci. Technol. **6**, 27 (1991).

Downloaded 13 May 2002 to 152.1.79.110. Redistribution subject to AIP license or copyright, see http://ojps.aip.org/japo/japcr.jsp